ELSEVIER

Journal of Power Sources 74 (1998) 68–76

JOURNAL OF POWER SOURCES

Thin lead dioxide electrodes for high current density applications in semi-bipolar batteries

Ingela Petersson *, Bo Berghult, Elisabet Ahlberg

Department of Inorganic Chemistry, Göteborg University, S-412 96 Göteborg, Sweden

Received 10 October 1997; revised 8 January 1998

Abstract

In the present paper, Planté-formed, thin-foil lead dioxide electrodes for applications in a semi-bipolar battery construction have been studied using impedance measurements, phase characterization and galvanostatic cycling. The effect of interparticle contact, IR-drop, porosity and mechanical pressure on the cell capacity were investigated in order to gain information about capacity-limiting parameters at high current discharges. The results showed that a more porous electrode received a capacity loss due to increased IR-drop, which in turn was caused by a decreased interparticle contact. The interparticle contact was found to be more important than porosity as a capacity-limiting factor. By exerting an external pressure over the cell, it was possible to increase the initial capacity for high current density discharges.

Keywords: Lead acid batteries; Thin electrodes; High current discharges; Impedance spectroscopy; IR-drop; Porosity; Mechanical pressure

1. Introduction

Due to its low resistance and high specific power, a bipolar battery construction of the lead acid battery system has been found to be well suited for high-power applications [1]. An interesting and expanding area is the hybrid and electric vehicles, where high power for short discharge periods is especially important. The bipolar PbO_2/Pb system has been shown to have higher power density than any other rechargeable aqueous battery system [2,3]. From an economic viewpoint, the lead acid battery is a cost-effective alternative, and, though 150 years old, still has the potential for further improvements. Many bipolar lead acid battery systems have been described in detail in the literature [1–10].

The work presented in this paper is based on a concept of a semi-bipolar battery described by Sundberg and Nilsson [11]. Here, the electrodes are made monopolar, assembled into two electrode units and joined in such a way that a bipolar or a semi-bipolar battery pile is formed.

The material utilization at high current density discharges is not high enough if tubular, or pasted lead dioxide electrodes, are used. One way to eliminate this problem is to use thin electrodes, which can be constructed using Planté formation, an electrochemical reduction–oxidation of lead foils.

The aim of the present work was to characterize Planté-formed, thin-foil, semi-bipolar lead dioxide electrodes for discharge times from milliseconds to a few minutes with respect to capacity during galvanostatic charge and discharge cycling. As a complement to the galvanostatic parameter study, A.C. impedance measurements were made to study changes in resistance and porosity at different potentials in the $PbSO_4/PbO_2$ region. In addition, phase characterization, i.e., porosity and compact density measurements were conducted during different steps in the process.

The use of electrochemical methods to create both a conducting substrate and the active material was shown to be an effective method to obtain thin, stable and functional electrodes in a relatively simple way. In addition, the unhealthy handling of lead oxides can be eliminated, and the electrodes can be constructed using techniques well known in the electroplating industry. Since the discharge capacity is often limited by the positive electrode, this study will focus on the aspects of the lead dioxide electrode. Many parameters can influence the final capacity; thus, it is of importance to study the parameters that have

* Corresponding author.

0378-7753/98/$19.00

the largest influence on the cell capacity and find the most suitable alternative for the particular application. In this investigation, the IR-drop, porosity and the mechanical pressure were studied. The balance between a thicker, porous electrode or a thinner, and more compact electrode has to be considered for each application with respect to weight, stability and corrosion.

At high current discharges and short discharge times, there is no need for an excess of electrolyte in the cell, since the electrode reactions are so rapid as to make the process limited by resistance to diffusion [8,12]. In several papers, increasing the cycle life by exerting a mechanical pressure on the electrodes have been reported [13–18]. Increased interparticle contact, non-shedding, as well as improved contact between the grid and the active material, are other positive effects reported of a pressurized cell. In these investigations, complete cells with commercial electrodes and separators were used, and many of the mentioned effects are therefore attributed to the traditional lead acid battery. In the present study, the effect of external pressure on the initial capacity of a single semi-bipolar cell was investigated. The reason for choosing this parameter was to find out if an external pressure would influence the initial capacity of the semi-bipolar electrodes at high power discharges.

2. Experimental

2.1. Electrodes and capacity measurements

The semi-bipolar electrodes ($\varnothing = 24$ mm) were prepared by electroplating lead through a glass substrate. The glass substrate (Fig. 1a) was constructed from about 175 capillary tubes moulded in epoxy in a PVC tube and cut into 2–5 mm thick matrices. A 500-μm thin lead foil (99.95%, Good Fellow) was attached to the back of the glass substrate, and lead was then electrochemically precipitated into the pore system of the substrate in a methane sulphonic acid electrolyte. The electroplating process was performed in the cell type shown in Fig. 1b. The process were continued until a layer of hemispheric lead was seen on the side opposite to the lead foil. This technique was used in order to create thin electrodes with even current distribution and good contact, and is described in detail in Ref. [19]. The anode was constructed using a pure 150 μm lead foil (Jung & Lindig), and the cathode was the semi-bipolar electrode described here. A PVC separator was used in this experiment to avoid shedding from the anode to the cathode surface.

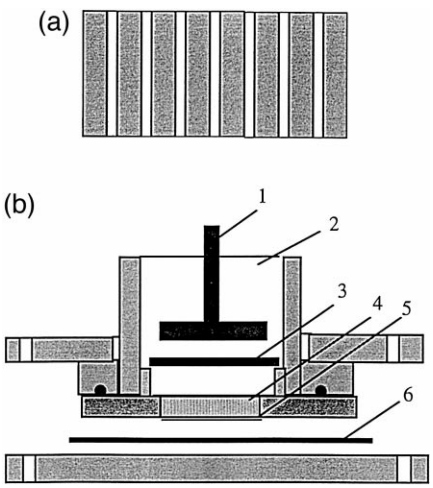

Fig. 1. (a) Cross-section of the glass substrate. (b) Cross-section of a cell for galvanostatic electroplating of lead. (1) Anode, (2) Electrolyte, (3) Separator, (4) Glass substrate, (5) Lead foil, (6) Current conductor.

In the next step, the lead foil was converted to active material, lead dioxide and spongy lead (Pb^*) by an electrochemical oxidation–reduction process, the Planté formation. The Planté formation process can be described by the following sequences for the positive electrode,

$$Pb \xrightarrow[1]{H_2SO_4 + KClO_4} PbO_2 \xrightarrow[2]{H_2SO_4 + KClO_4} Pb^* \xrightarrow[3]{H_2SO_4} PbO_2 \quad (1)$$

and for the negative electrode,

$$Pb \xrightarrow[1]{H_2SO_4 + KClO_4} PbO_2 \xrightarrow[2]{H_2SO_4 + KClO_4} Pb^* \quad (2)$$

Positive electrodes consisting of active material corresponding to 100, 200 and 400 μm conversion of the lead foil were made. To obtain the different thicknesses, the same current density was used while the formation time was changed. The weight of the electrodes before and after each formation was used to determine the current utilization. The results from this gravimetric measurement showed that the formation process was performed with almost 100% conversion [20]. The electrodes will be referred to as the thicknesses 100, 200 and 400 μm for the remainder of the text.

The positive electrodes were washed in 8 M HNO_3 (p.a., Merck) and rinsed in deionized milli-Q water before being used. The foils were pretreated for about 30 min at 1.5 mA cm^{-2} in a cathodic process where air formed lead oxides is reduced to lead in an electrolyte consisting of 0.5 M H_2SO_4 and 0.05 M $KClO_4$. Lead dioxide was then formed and reduced with 10 mA cm^{-2} in the same electrolyte. After the reduction process, the perchlorate ions were rinsed from the electrodes, and the spongy lead on the positive electrode was oxidized to lead dioxide in pure 1 M H_2SO_4. A porous polyester and a PVC separator were used to support the positive active material in this process.

After the formation process, the electrodes were assembled to (2V) laboratory cells and characterized galvanostatically. The characterization studies were performed in the cell type shown in Fig. 2. However, in the experiments where an external mechanical pressure was exerted on the

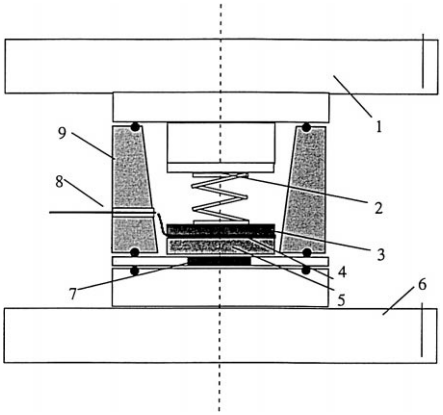

Fig. 2. Cross-section of a cell for Planté formation and cell characterization. (1) PVC plate, (2) Spring, (3) Negative active material, (4) Current conductor, (5) Separator, (6) PVC plate, (7) Positive active material, (8) Gas vent and reference electrode (9) PVC cylinder.

electrodes, a cell of the type shown in Fig. 3 was used. This cell was very similar to the one shown in Fig. 2 with the following exception. A cylinder with an adjustable spring was placed on top of the bolts (Fig. 3). The mechanical pressure was applied by exerting a force on the cylinder to the desirable pressure and then locking it in place with a screwnut. The pressure could be determined by measuring the compression of the spring. Both constructions allows gas formed during the cycling to escape from the cell. The semi-bipolar electrodes were used as working electrodes and a conventional pasted lead electrode (Tudor Nol, Sweden) as counter electrode. A double junction $Ag/AgCl/KCl/K_2SO_4$ reference electrode and 5 M H_2SO_4 (p.a., Merck) electrolyte were used in all experiments. For the experiments conducted with an excess amount of electrolyte, two different separators were used, one polyester and one PVC, while for the experiment performed with a limited amount of electrolyte, only a high porous microglass fiber separator was used. Before measurement, the active material was stabilized by three discharges at 22 mA cm^{-2} in 5 M H_2SO_4. The electrodes

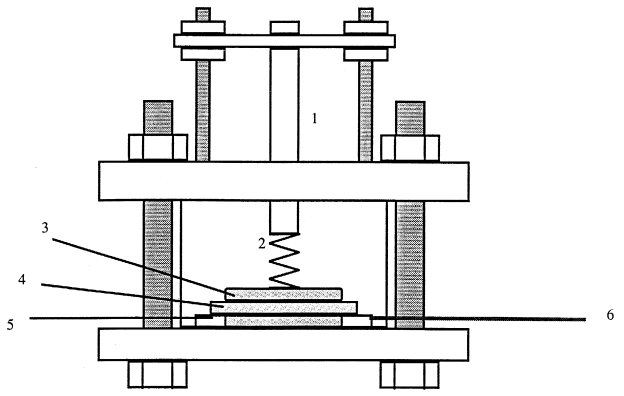

Fig. 3. Cross-section of a pressurized cell. (1) PVC-cylinder, (2) Spring, (3) Negative active material, (4) Separator, (5) Positive active material, (6) Reference electrode.

were examined by studying one parameter at a time measuring the positive and the negative electrode potential, as well as the discharge time and discharge current for each cell using a computerized control system. A number of discharges with different discharge currents (22–1000 mA cm^{-2}) were made to characterize the positive electrodes.

The IR-drop was measured before each discharge using a constant current step technique, where a current step of 500 mA was applied onto the cells, and the momental potential measured. This method was verified with impedance measurements using an EG&G, PAR (Princeton Applied Research) potentiostat/galvanostat model 273A and a Schlumberger HF frequency response analyzer SI1255.

2.2. The impedance study

In the present study, A.C. impedance measurements were made in order to obtain information about the changes in resistance and porosity. In the preliminary investigation, a wide potential region was investigated, ranging from −0.6 to 1.5 V in the $PbSO_4/PbO_2$ reaction. At a constant potential, a frequency sweep from 100 kHz to 2 mHz was used with an amplitude of the applied sine wave of 5 mV rms. Impedance spectra were taken at these different potentials as a function of the thickness of the preformed oxide layer and of the mechanical pressure.

The impedance diagrams was divided into two sections (Fig. 4) with the low-frequency data fitted by regression to a semicircle and the high-frequency data to a straight line [21–23].

From these data, the ohmic resistance and the pore resistance could be determined (Fig. 4).

2.3. Phase characterization

Phase characterization of the porous electrodes at different steps in the process were made in order to obtain information about the porosity and the internal surface area. The techniques used were SEM, BET, porosity and compact density measurements. The open porosity was calculated from the weight difference between the sample

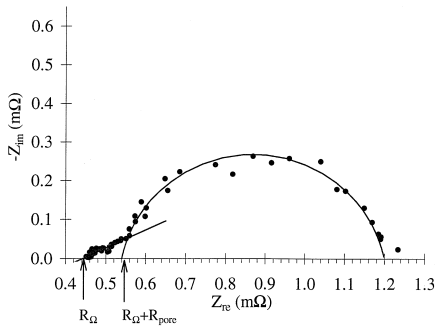

Fig. 4. Schematic picture of an impedance diagram used for evaluation of the impedance measurements.

Table 1
Electrode porosity determined by water intrusion

Thickness (μm)	Porosity (%)
100	14
200	19
400	27

in air and when suspended in water. The sample was initially dry-weighed and put under vacuum for at least 30 min. While under vacuum, the sample was covered with distilled water for 12 h. The wet weight of the sample was measured both in air and suspended in water. From this information, the exterior volume, bulk density and apparent porosity was calculated. The results were compensated for the metal foil. The porosity was determined after the complete formation, i.e., following step (3) in the formation process, and the results from this measurement is shown in Table 1. From SEM investigations of cross-sections of the different lead dioxide electrodes, it was shown that the porosity of the layer was homogeneous [20].

All experiments were carried out at room temperature.

3. Results and discussion

Positive electrodes consisting of 100, 200 respective 400 μm active material were discharged at current densities ranging between 22 and 1100 mA cm^{-2} with an excess of electrolyte (Fig. 5). From the discharge curves, it was clear that the discharge time increased with increasing active material thickness, i.e., $400 > 200 > 100$ μm and also that the capacity decreased with an increased discharge rate. A traditional way of representing these kind of data is according to the Peukert equation [24].

$$I^n \cdot t = C \quad (3)$$

where I is the current, t is the discharge time and n and C are constants. The constant n is an empirical constant that

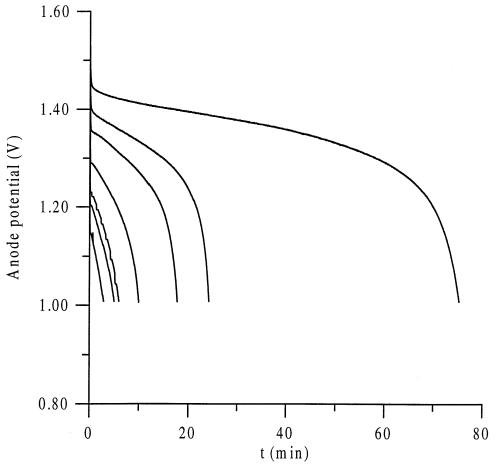

Fig. 5. Discharge curves at 22, 44, 66, 111, 155, 177 and 221 mA cm^{-2}, for a 100-μm electrode.

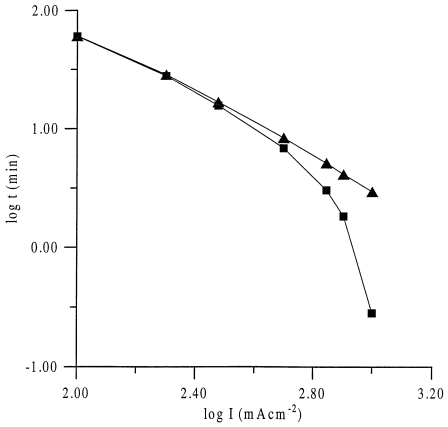

Fig. 6. Peukert curves for a 100-μm electrode (■) the uncompensated and (▲) the IR-compensated curves.

includes several parameters that influence the cell capacity, e.g., pore diffusion, pore blocking and electrolyte exhaustion. For the ideal case, where $n = 1$, there is no current dependence and C will be equal to the charge of the cell. Typically, n has a value between 1 and 2.

In this work, a modified version of Eq. (3) is used to compensate for the IR-losses,

$$I^n \cdot (t + t') = C \quad (4)$$

where t' corresponds to the additional discharge time caused by the elimination of the IR-drop.

In Fig. 6, two Peukert curves are compared: (i) the uncompensated and (ii) the compensated curves. The former bends at high current densities while the compensated line remains straight for all current densities.

3.1. IR-drop

The ohmic resistance of a cell is often discussed in terms of the resistance of the electrolyte. The effects are proportional to the current density and is most severe for high current densities. By careful measurements of the IR-drop, proper corrections can be made in order to determine the influence of the pure internal resistance on the cell capacity. The data is also useful when analyzing the different contributions to the total IR-drop. Measurements of the IR-drop for the semi-bipolar lead dioxide electrodes were made before each discharge.

In Fig. 4, a typical impedance spectrum is shown. The high-frequency cut-off corresponds to a combination of the solution resistance between the reference electrode and the surface of the electrode, R_Ω, and the electric resistance in the electrode. The high-frequency cut-off of the semi-circle corresponds to the solution resistance inside the pores, R_{pore}. For a porous electrode the high-frequency cut-off will decrease as the porosity increases, provided that the internal electric resistance of the electrode is minor. In the present case, however, the high-frequency cut-off increases

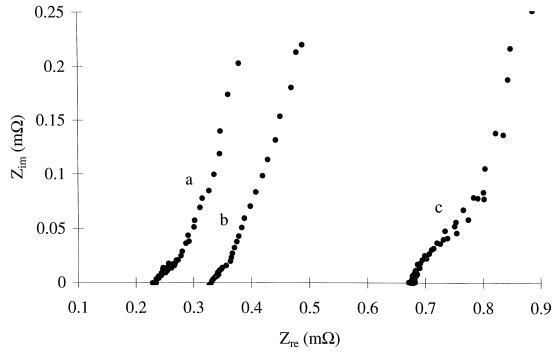

Fig. 7. Impedance diagrams illustrating the high-frequency cut-off for the three different formed lead foils, (a) 100 μm, (b) 200 μm and (c) 400 μm.

with the active material thickness, indicating an increase of the electric resistance (Fig. 7).

From the impedance diagrams, it can be seen that the IR-drop consisted of more than one resistance component. This is illustrated in Fig. 8, where the IR-drop is plotted as a function of the thickness of the oxide layer. It can be seen that the total IR-drop consists of contributions from R_{pore} and R_{Ω}. R_{pore} is related to the porosity of the oxide layer. R_{Ω} can be divided into two parts; (i) the resistance of the electrolyte and (ii) the degree of contact between the lead dioxide particles in the material. The total ohmic resistance for the three different electrodes were found to be 0.4–0.7 (400 μm), 0.3–0.34 (200 μm) and 0.26–0.28 Ω for the 100 μm foil. The range in values originates from approximately 10 different experiments. Although the resistance increased with an increasing amount of lead dioxide in the electrodes, which is in agreement with the literature [2,8,25], the contributions from the porosity and the electrolyte resistance are small compared to the contribution from the interparticle contact to the total IR-drop. In the more porous 400 μm electrode, the interparticle contact cannot be as good as in the less porous 100 μm electrode, resulting in a larger IR-drop. Using a current density of 1100 mA cm^{-2}, about 80% of the active material for a 100 μm electrode remains unreacted due to IR-losses. The major part of the IR-loss is due to the lack of interparticle contact, while the electrolyte resistance only accounts for a small percentage of the total loss. This is due to the high concentration of the sulphuric acid (5 M) used in the experiment. In addition, the influence of the porosity is minimal and more or less constant through the experiment. The porosity will be discussed in more detail below. In order to further evaluate other capacity limiting effects such as pore diffusion, pore blocking and electrolyte exhaustion, the data obtained from the IR-drop experiments was evaluated to retrieve the IR-free capacities of the positive electrode.

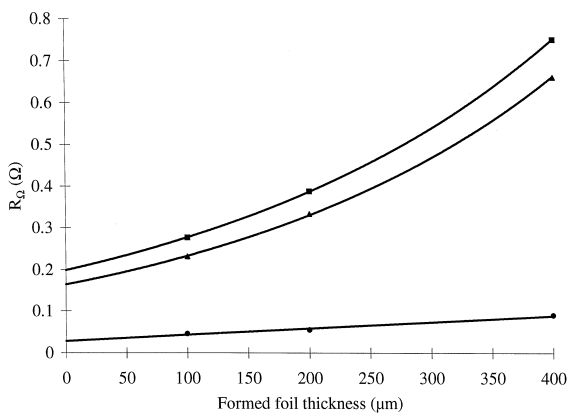

Fig. 8. Ohmic resistance as a function of formed foil thickness, (■) $R_{\Omega} + R_{pore}$, (▲) R_{Ω}, and (·) R_{pore}.

3.2. Current utilization

The IR-compensated current utilization as a function of the positive active material (PAM, 0.2241 Ah g^{-1}) for four different current densities (22, 111, 221 and 1100 mA cm^{-2}) can be seen in Fig. 9. In Fig. 10, the corresponding current utilizations are shown for the same formed foil thicknesses, but with the amount of electrolyte limited with respect to the amount present in the active material itself, and in one of the porous microglass separators. As can be seen in Fig. 9, current utilization increases with thinner active material thickness, which is also in agreement with the literature [2,8,25]. From Fig. 10, it can be concluded that the current utilization is reduced compared to the case where an excess of electrolyte was used. This may be explained by either pore diffusion or pore blocking.

The IR-compensated Peukert curves for the positive electrode with and without an excess of electrolyte are shown in Fig. 11. It is interesting to note from this figure that for the higher current densities in excess of electrolyte, the values of the capacity approach each other, indicating that there is no difference in the discharge times for the

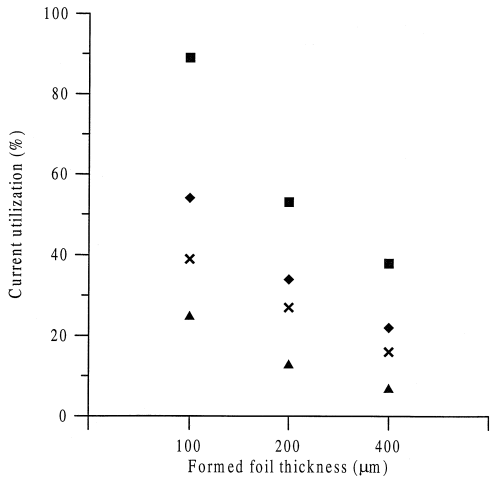

Fig. 9. The IR-compensated current utilization as a function of formed foil thickness using an excess of electrolyte, (■) 22 mA cm^{-2}, (◆) 111 mA cm^{-2}, (×) 221 mA cm^{-2} and (▲) 1100 mA cm^{-2}.

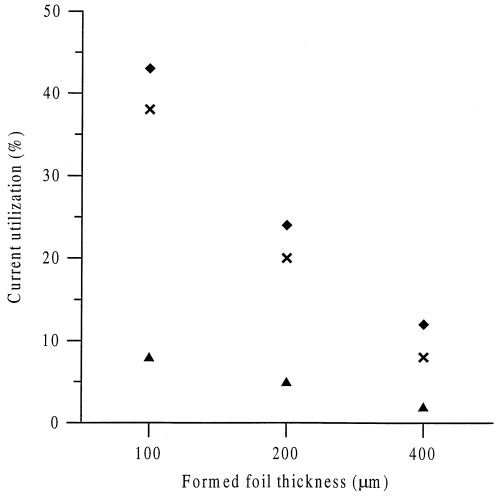

Fig. 10. The IR-compensated current utilization as a function of formed foil thickness with a limited amount of electrolyte, (♦) 111 mA cm^{-2}, (×) 221 mA cm^{-2} and (▲) 1100 mA cm^{-2}.

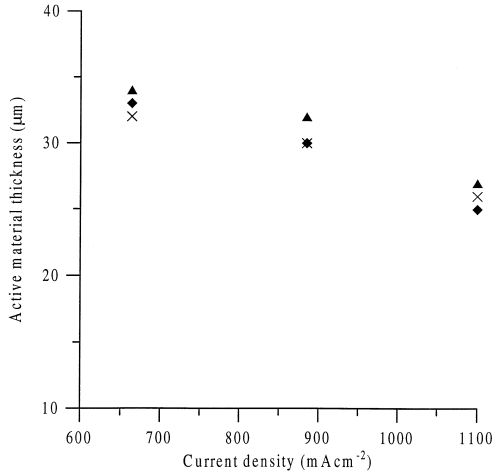

Fig. 12. Amount of utilized active material as a function of discharge current density, (♦) 100 μm, (×) 200 μm, and (▲) 400 μm.

three active material thicknesses, i.e., only the very front of the electrodes are discharged, and not the deeper regions. From Fig. 11, it was calculated that as much as 84 (400 μm), 73 (200 μm) and 61 (100 μm) % of the lead dioxide was left unreduced when a current density of 221 mA cm^{-2} was used. In Fig. 12, the amount of utilized active material during three different high current discharges (664, 885 and 1100 mA cm^{-2}) is shown as a function of discharge current density. It can be seen in this figure that for all the three electrodes at these current densities, the utilized active material thickness is about 30 μm. These similarities in current utilization and amount of utilized active material for the three different electrode thicknesses, especially for high current discharges, are probably due either to electrolyte depletion or to rapid formation of lead sulfate on the surface of the active material. When the electrodes are discharged and $PbSO_4$ begins to precipitate by nucleation, the insulating lead sulfate plugs the pores and prevents further reaction, leaving an unreduced core of PbO_2. As the current densities are increased, the passivation reaction becomes faster due to the formation of much smaller $PbSO_4$ crystals, resulting in a higher degree of coverage [26–29]. It can be concluded that the amount of PbO_2 left unreduced would be minimized if the electrodes were made even thinner as shown in this study.

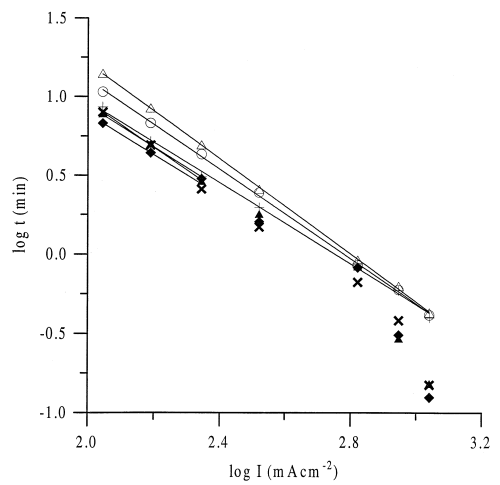

Fig. 11. IR-compensated Peukert curves for the three different electrode thicknesses using an excess of electrolyte, (△) 100 μm, (○) 200 μm, (+) 400 μm and with the amount of electrolyte limited, (×) 100 μm, (▲) 200 μm and (■) 400 μm.

From the Peukert curves in Fig. 11, where the amount of electrolyte is limited, the cells become more or less exhausted above a current density of 221 mA cm^{-2}. This can be explained by depletion of electrolyte close to the reaction sites, and indicates that for the same current densities, more lead dioxide is left unreduced than was found in the experiments using an excess amount of electrolyte. It is thus reasonable to conclude that the limiting factor in these experiments seems to be the exhaustion of electrolyte close to the active material. When the amount of electrolyte was doubled, no big differences in discharge time was found for any of the three electrodes. A similar result was found when the amount of electrolyte was increased by a factor of three and four. It is also clear from the experiment that no more electrolyte than is absorbed in one microporous glass separator, i.e., 0.546 ml, together with the amount present in the positive material itself 0.018 (100 μm), 0.042 (200 μm) and 0.106 ml (400 μm), can be used before the process is limited by pore diffusion or passivation. Calculations of the pulsed discharge behavior of thin cells made by LaFollette and Bennion [3] showed that during the first 200 μs, the current is limited by depletion of acid close to the electrode surface, after which the passivation reaction becomes limiting. When the electrolyte is consumed and further reaction is limited by pore diffusion, the pH increases close to the active material and unwanted products, such as

basic lead sulfates, and lead oxides may be formed, limiting further reaction. Another plausible explanation is pore plugging by $PbSO_4$ where the reactions are not limited by electrolyte access.

3.3. Porosity

In order to determine the capacity-limiting effects of the lead dioxide electrodes, the porosity has to be considered as a factor that influences the capacity. A more porous electrode structure can hold more electrolyte, and therefore avoid electrolyte exhaustion as a capacity-limiting effect. Porosity and compact density measurements of the three different material thicknesses used in this study was made in order to gain valuable information about the properties and the behavior of the porous lead dioxide electrode.

The electrodes were found to have porosities of about 27% for 400, 19% for 200 and 14% for 100 μm thickness (Table 1). Although there was a difference in porosity between the three electrodes, the pore resistance was small compared to the overall resistance; therefore, it is clear that the porosity cannot be the main contribution to the large resistance term. Instead, it was seen from the impedance diagrams that the contact between the particles in the electrode seems to be an important aspect for the capacity of the cell. The less porous the active material, the better is the chance for good interparticle contact. Imperfections in the contact pattern between the particles may result in difficulties for electron movement, necessary for discharging. From this study, it was shown that thicker electrodes resulted in reduced discharge capacity. The most porous electrode, the 400 μm electrode, showed the smallest current utilization while the less porous 100 μm showed the highest.

From the impedance study, it was deduced that the porosity was not preserved during the formation, but instead the geometry of the pores changes. The results from the impedance study showed no increase in resistance during the formation, and since the pores become longer during the process, it is likely that the pores also become wider.

In the literature, the discharge capacity and porosity of the lead dioxide electrodes is often discussed with respect to the ratio of the two lead dioxide phases, α- and β-PbO_2, in the electrodes. It is generally believed that of the two different phases, the α-PbO_2 has a more compact structure, resulting in a better contact between the particles [30–32]. However, a combination of the two phases, where the α-PbO_2 preserve the electronic contact and the β-PbO_2 gives high discharge capacity, would be an ideal electrode.

In the present study it is shown that a thinner, less porous electrode have a higher discharge capacity than a thicker, more porous electrode. The increase in discharge capacity may be explained by a higher degree of α-PbO_2 in the thinner electrodes compared to a thicker and more porous electrode. This has been proposed earlier by Ahlberg and Berghult [30], who suggested that different cations influence the structure of electrochemically formed lead dioxide. It was also suggested in this work that the size of different cations in the perchlorate-assisted formation of PbO_2 may influence the ratio between α- and β-PbO_2, but no structural evidence was given. A more detailed investigation concerning structural investigation of PbO_2 formed with different perchlorate salts during the Planté formation process was therefore initiated, and the results will be presented in a forthcoming paper [20].

3.4. Mechanical pressure

A mechanical pressure exerted over the cell have been reported to increase its cycle life [13–18]. In the present work, the effect of external pressure on the capacity at high power discharges was studied. When different mechanical pressures (1.5, 3.5 and 5 kg cm^{-2}) was exerted over the cells, it was seen that the pressure initially increased the capacity of the lead dioxide electrodes for high current density discharges. In Table 2, the current utilization (%) for the three electrode thicknesses as a function of current density, amount of electrolyte and different mechanical pressures is shown. Thus, from Table 2, it can be seen that the capacity for all the three electrodes was largest when mechanical pressure of 3.5 kg cm^{-2} was exerted over the cells and lowest when about 1 kg cm^{-2} was used. According to the literature [13–18], the optimal pressure for increasing the cycle life of a battery was 10^5 Pa corresponding to $\sim$1 kg cm^{-2}.

From the Peukert curves in Fig. 13, where five different experimental conditions are compared for the 200-μm

Table 2
Current utilization for the three electrode thicknesses as a function of current density, amount of electrolyte and mechanical pressure over the cell

Limited amount of electrolyte	100 μm	200 μm	400 μm
Current density (111 mA cm^{-2})			
$\sim$1 kg cm^{-2}	43	24	12
1.5 kg cm^{-2}	43	30	17
3.5 kg cm^{-2}	55	33	26
5 kg cm^{-2}	44	26	28
Excess of electrolyte	54	34	22
Current density (221 mA cm^{-2})			
$\sim$1 kg cm^{-2}	38	18	8
1.5 kg cm	39	26	16
3.5 kg cm^{-2}	39	26	21
5 kg cm^{-2}	32	26	27
Excess of electrolyte	39	27	16
Current density (1100 mA cm^{-2})			
$\sim$1 kg cm^{-2}	8	5	2
1.5 cm^{-2}	13	8	4
3.5 kg cm^{-2}	20	16	9
5 kg cm^{-2}	14	12	6
Excess of electrolyte	25	13	7

electrode, it can be seen that when the cell was pressurized, the capacity of the electrodes was preserved even during the highest current densities, while the electrodes lose their capacity in the case where a limited amount of electrolyte was used. When the pressure was increased to 5 kg cm^{-2}, the capacity was slightly reduced, especially for the higher current densities.

The 100-μm electrode showed about the same behavior as the 200 μm electrode with a few exceptions. This electrode showed no increasing capacity when a low, 1.5 kg cm^{-2}, or the highest i.e., 5 kg cm^{-2} pressure was exerted over the cell. This is in contrast to the results obtained for cells with an excess of electrolyte. However, the *n*-value for the 100-μm electrode indicates that the active material was quite well utilized and not very sensible to external pressure. The *n*-values for the 200-μm electrode indicate that the capacity of the 200-μm electrode increased to a greater extent than the 100-μm electrode by pressurizing.

The 400-μm electrode showed a slightly different behavior compared to the 100- and 200-μm electrodes. For the 400-μm electrode, the Peukert lines are quite well separated, and higher *n*-values indicate that a thinner part of the active material was utilized in these electrodes. However, the largest differences for this electrode compared to the other two was seen when the highest pressure, 5 kg cm^{-2} was exerted over the cell. For this electrode, the capacity continued to increase with a higher pressure for current densities up to 221 mA cm^{-2}.

Impedance measurements were conducted for all electrode thicknesses and current densities. The results from this study was used to verify the results from the galvanostatic electrode characterization. The results showed that for the most porous oxide layer at negative potentials, the dispersion factor, α was about ≤ 0.5, which is the expected behaviour for a conducting porous electrode. At these potentials, there was no clear dependence on pressure. At slightly positive overpotentials, α depends on the pressure, with the lowest α found for cells without extended pressure. At the highest pressures, α approaches 1 for electrode thicknesses of 400 and 200 μm. This indicates that the oxide layer collapses, and that the porous active area decreases. For the 100-μm layer, the influence of pressure on α was not as clear as for the more porous layer. These results indicate that changes in α can be correlated to the porosity of the layer.

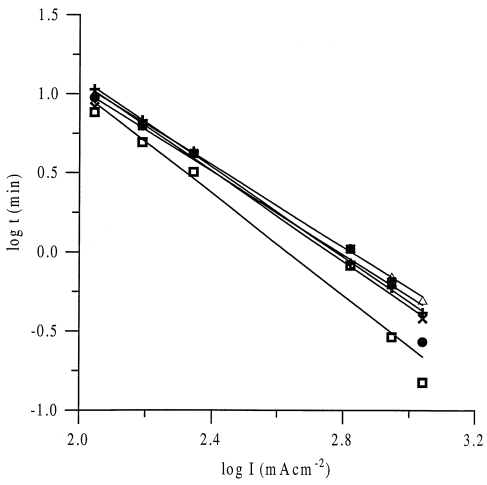

Fig. 13. IR-compensated Peukert curves for a 200-μm electrode during the five different experimental parameters, (+) excess of electrolyte, (□) limited amount of electrolyte, (○) 1.5 kg cm^{-2} (△) 3.5 kg cm^{-2} (×) 5 kg cm^{-2}.

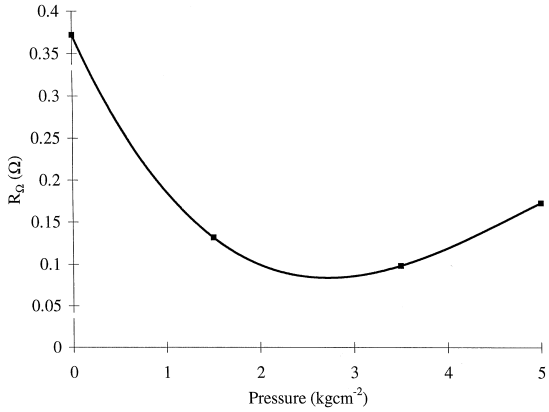

Fig. 14. Total ohmic resistance as a function of mechanical pressure for a 200-μm electrode.

The results from the pressurized cells indicate that the increased capacity was due to some kind of interparticle contact effect, since the mechanical pressure influenced the capacity of the thicker and more porous electrodes more than the thinner electrodes. Indeed, the ohmic resistance was reduced with an increased pressure and increased when the pressure was removed. In Fig. 14, the total ohmic resistance is plotted as a function of the mechanical pressure for a 200-μm electrode. In this figure, it is seen that the ohmic resistance decreases with an increasing mechanical pressure to a certain value between 1.5–3.5 kg cm^{-2}, where the ohmic resistance began to rise again. The distribution of the ohmic resistance between R_{pore} and R_{Ω} is about the same as seen in Fig. 9, where the ohmic drop was plotted as a function of the thickness of the oxide layer, which also was expected because of the increased contact between the particles when a mechanical pressure is exerted over the cells. Thus, when the pressure becomes too high, the material collapses and the lead dioxide structure is destroyed. In addition, the mechanical pressure may force the electrolyte out of the material during cycling, and therefore a better contact between the particles does not result in an improvement of the capacity.

4. Conclusions

The main conclusions of this investigation can be summarized as follows.

● For high discharge currents, the ohmic resistance of a cell resulted in an increased capacity limitation. Using a current density of 1100 mA cm^{-2}, as much as 80% of the active material of a 100-μm electrode remains unreacted due to IR-drops.

● The total IR-drop was due to contributions from porosity, electrolyte and lack of interparticle contact, where the latter contributed the major part.

● The use of electrochemical methods to create both the conducting substrate and the active material was shown to be an effective method to create stable and functional electrodes in a relatively simple way. Besides, the unhealthy handling of lead oxides was eliminated and the electrodes were created using techniques well known in the electroplating industry.

● The use of thin and dense active material layers resulted in high material utilization and high discharge currents.

● By exerting an external pressure over the cell, it was possible to increase the initial capacity for high current density discharges. This was due to a decrease in the total ohmic resistance, and is most pronounced in the range between 1.5–3.5 kg cm^{-2}.

● By exerting pressure on the cell several things were noticed: (i) Increased interparticle contact; and (ii) Forcing of the electrolyte out of the material during cycling, when the structure of the active material was changed.

The most important result from the present study is that interparticle contact is more important than porosity as capacity-limiting effect.

Acknowledgements

This work has received financial support from the Swedish National Board for Industrial and Technical Development (NUTEK). The authors gratefully acknowledge Ove Nilsson for his support of this work.

References

[1] D.N. Bennion, Bipolar electrodes and the future of battery designs, Ext. Abstr., Proc. Electrochem. Soc., Pennington, NJ, USA, 92-2, 1992, p. 1.
[2] R.M. LaFollette, D.N. Bennion, J. Electrochem. Soc. 137 (1990) 3693.
[3] R.M. LaFollette, D.N. Bennion, J. Electrochem. Soc. 137 (1990) 3701.
[4] R.M. LaFollette, Design and Performance of High Specific Power, Pulsed Discharge, Bipolar Lead Acid Batteries, Proc. 10th (IEEE) Annual Battery Conference, 1995, p. 43.
[5] R.M. LaFollette, D.N. Bennion, Design Fundamentals of Very High Power Density, Pulse Discharge Lead Acid Batteries, Ext. Abstr., Proc. Electrochem. Soc., Pennington, NJ, USA, 1987, p. 40.
[6] A.I. Attia, J.J. Rowlette, The Development of a New Sealed Bipolar Lead-Acid Battery, Proc. 33rd Int, Power Sources Symp., Cherry Hill, NJ, USA, 1988, p. 624.
[7] J.L. Arias, J.J. Rowlette, E.D. Drake, Design Study of the Sealed Bipolar Lead-Acid Battery for Load Leveling Applications, Report, Arias Research Associates.
[8] W.-H. Kao, J. Power Sources 36 (1991) 155.
[9] M. Eskra, R. Vidas, R. Miles, G. Halpert, A. Attia, D. Perrone, Bipolar Lead Acid Battery Development, IECEC-91, Proceedings of 26th Intrersociety Energy Conversion Engineering Conference, 1991.
[10] K.R. Bullock, J. Electrochem. Soc. 142 (1995) 1726.
[11] E. Sundberg, O. Nilsson, Pat. Appl. PCT/SE 92/00493, (July 1, 1992).
[12] D. Simonsson, The Discharge Process of the Porous Lead Dioxide Electrode, PhD Thesis, Institutionen för kemisk teknologi Kungl. Tekniska Högskolan, Stockholm, Sweden, 1973.
[13] J. Landfors, J. Power Sources 52 (1994) 99.
[14] S. Atlung, B. Zachau-Christiansen, J. Power Sources 30 (1990) 131.
[15] J. Alzieu, J. Robert, J. Power Sources 13 (1984) 93–100.
[16] J. Alzieu, N. Koechlin, J. Robert, J. Electrochem. Soc. 134 (1987) 1881.
[17] K. Takahashi, M. Tsubota, K. Yonezu, K. Ando, J. Electrochem. Soc. 130 (1983) 2144.
[18] P. Herger, Planseeberichte fur Pulvermetallurgie 24 (1976) 284.
[19] O. Nilsson, I. Petersson, A high power density, semi-bipolar lead acid battery for electric hybrids, 19th International Power Sources Symposium, Brighton, UK, 1995, p. 183.
[20] I. Petersson, E. Ahlberg, B. Berghult, J. Power Sources, 1997, accepted.
[21] C. Cachet, R. Wiart, Electrochim. Acta 29 (1984) 145.
[22] J.-P. Candy, P. Fouilloux, Electrochim. Acta 27 (1982) 1585.
[23] J.-P. Candy, P. Fouilloux, Electrochim. Acta 26 (1981) 1029.
[24] W.Z. Peukert, Electrochemistry 18 (1897) 287.
[25] B. Berghult, Fundamental Electrochemical Aspects of the Lead Electrode in Connection with the Lead-Acid Battery, PhD Thesis, Department of Inorganic Chemistry Chalmers University of Technology and the University of Göteborg, Göteborg, Sweden, 1990.
[26] P. Casson, N.A. Hampson, K. Peters, P.J. Whyatt, Appl. Electrochem. 7 (1977) 257.
[27] A.C. Simon, S.M. Caulder, J.T. Stemmle, J. Electrochem. Soc. 122 (1975) 461.
[28] J.L. Weininger, C.R. Morelock, J. Electrochem. Soc. 122 (1975) 1161.
[29] S. Hattori, M. Yamaura, M. Kohno, Y. Ohtani, M. Yamane, H. Nakashima, Periodic observation of the same pin-point of battery plates with the scanning electron microscope, Power Sources 5, Academic Press, London, 1975, p. 139.
[30] E. Ahlberg, B. Berghult, J. Power Sources 32 (1990) 243.
[31] P. Ruetschi, J. Electrochem. Soc. 139 (1992) 1347.
[32] E. Voss, J. Freundlich, Discharge Capacities of Alpha and Beta Lead Dioxide Electrodes, Batteries, D.H. Collins (Ed.), Pergamon, Oxford, 1963, pp. 73.